Biochimica et Biophysica Acta 1840 (2014) 556–564

Contents lists available at ScienceDirect

Biochimica et Biophysica Acta

journal homepage: www.elsevier.com/locate/bbagen

Depletion of casein kinase I leads to a NAD(P)$^+$/NAD(P)H balance-dependent metabolic adaptation as determined by NMR spectroscopy-metabolomic profile in *Kluyveromyces lactis*

D. Gorietti [a], E. Zanni [b], C. Palleschi [b], M. Delfini [a], D. Uccelletti [b,*], M. Saliola [b,**], A. Miccheli [a]

[a] Department of Chemistry, Sapienza University of Rome, Piazzale A. Moro 5, 00185 Rome, Italy
[b] Department of Biology and Biotechnology C. Darwin, Sapienza University of Rome, Piazzale A. Moro 5, 00185 Rome, Italy

ARTICLE INFO

Article history:
Received 26 June 2013
Received in revised form 25 September 2013
Accepted 12 October 2013
Available online 18 October 2013

Keywords:
Yeast
Metabolomics
Casein kinase
NAD(P)$^+$/NAD(P)H balance
NMR spectroscopy

ABSTRACT

Background: In the Crabtree-negative *Kluyveromyces lactis* yeast the *rag8* mutant is one of nineteen complementation groups constituting the fermentative-deficient model equivalent to the *Saccharomyces cerevisiae* respiratory *petite* mutants. These mutants display pleiotropic defects in membrane fatty acids and/or cell walls, osmo-sensitivity and the inability to grow under strictly anaerobic conditions (Rag$^-$ phenotype). *RAG8* is an essential gene coding for the casein kinase I, an evolutionary conserved activity involved in a wide range of cellular processes coordinating morphogenesis and glycolytic flux with glucose/oxygen sensing.
Methods: A metabolomic approach was performed by NMR spectroscopy to investigate how the broad physiological roles of Rag8, taken as a model for all *rag* mutants, coordinate cellular responses.
Results: Statistical analysis of metabolomic data showed a significant increase in the level of metabolites in reactions directly involved in the reoxidation of the NAD(P)H in *rag8* mutant samples with respect to the wild type ones. We also observed an increased *de novo* synthesis of nicotinamide adenine dinucleotide. On the contrary, the production of metabolites in pathways leading to the reduction of the cofactors was reduced.
Conclusions: The changes in metabolite levels in *rag8* showed a metabolic adaptation that is determined by the intracellular NAD(P)$^+$/NAD(P)H redox balance state.
General significance: The inadequate glycolytic flux of the mutant leads to a reduced/asymmetric distribution of acetyl-CoA to the different cellular compartments with loss of the fatty acid dynamic respiratory/fermentative adaptive balance response.

1. Introduction

All eukaryotes have the ability to detect and respond to environmental signals. Adaptation to stress/environmental conditions occurs in single-cell organisms triggering a large common transcriptional response, called in yeast environmental stress response [1]. Its knowledge is crucial for the understanding of environmental and physiological adaptation of the cells during their use in biotechnological applications.

Since *Kluyveromyces lactis* is an attractive host alternative to *S. cerevisiae* for heterologous protein production, for a current review on the topic see [2], fundamental knowledge about its adaptive mechanisms is thus a prerequisite to optimize conditions for large-scale biomass production. *K. lactis* is a Crabtree-negative yeast in which both respiratory and fermentative pathways co-exist during growth on glucose [3–5], although respiration appears to be dispensable since antimycin A does not inhibit growth on glucose (Rag$^+$ phenotype) [6,7]. We previously reported that *rag* mutants (Rag$^-$ phenotype) also displayed sensitivity to osmotic stress conditions, constitutive activation of the Hog pathway as well as altered fatty acid content and cell wall functionality and, therefore, unable to accumulate/produce glycerol. These data suggested that a common pathway regulates glucose utilization and stress response mechanisms in all *rag* mutants [8]. Among them, *RAG8* is an essential *K. lactis* gene coding for the casein kinase I isoform (CKI) involved in the transcriptional regulation of the low-affinity glucose transporter gene *RAG1* [9]. It has also been reported that Rag8 controls the transcription factor Sck1 by transcriptional and post-translational regulations, coordinating glucose transport and glycolysis [10]. In *S. cerevisiae*, CKI is a serine/threonine protein kinase playing important regulatory roles, as suggested by the widespread distribution of CKI isoforms encoded by four distinct genes, *YCK1*, *YCK2*, *YCK3* and *HRR25* [11–13]. Yck proteins have been shown to play a role in morphogenesis [14], in vesicle transport [13,15], in the

* Correspondence to: D. Uccelletti, Dept. Biology and Biotechnology, Sapienza University of Rome, P.le A. Moro 5, 00185 Rome, Italy. Tel.: +39 0649912258; fax: +39 0649912351.
** Correspondence to: M. Saliola, Dept. Biology and Biotechnology, Sapienza University of Rome, P.le A. Moro 5, 00185 Rome, Italy. Tel.: +39 064 991 2254; fax: +39 064 991 2351.
E-mail addresses: daniela.gorietti@uniroma1.it (D. Gorietti), elena.zanni@uniroma1.it (E. Zanni), claudio.palleschi@uniroma1.it (C. Palleschi), maurizio.delfini@uniroma1.it (M. Delfini), daniela.uccelletti@uniroma1.it (D. Uccelletti), michele.saliola@uniroma1.it (M. Saliola), alfredo.miccheli@uniroma1.it (A. Miccheli).

0304-4165/$ – see front matter © 2013 Elsevier B.V. All rights reserved.
http://dx.doi.org/10.1016/j.bbagen.2013.10.020

phosphorylation of plasma membrane H^+ ATPase [16] and in the ubiquitination and internalisation of uracil permease [17]. Recently, a role for Yck1 and Yck2 in superoxide dismutase-dependent respiration repression has also been found. Apparently, the reaction catalyzed by Sod1 promotes Yck1 stability as well as glucose and O_2 sensing, by controlling the amount of superoxide conversion to peroxide. In this manner, in a single circuit, O_2, glucose, and reactive oxygen species can repress respiration through Sod1/CKI signaling [18].

Given the broad physiological roles of Rag8, we investigated the metabolic changes taking place in mutant cells under stress conditions, when they are no longer able to induce membrane adaptations. To address this question and to globally characterize the metabolic responses of *K. lactis* to the lack of the CKI, a NMR-based metabolomic approach was employed.

2. Materials and methods

2.1. Strains, media and culture conditions

The strains used in this study are listed in Table 1. Cultures were grown under shaking conditions at 28 °C in YP (1% Difco yeast extract, 2% Difco Bacto-peptone) supplemented with glucose at the concentration of 0.5 g/L. When the cells reached 0.7 OD_{600}, glucose was added to the medium at 1.6 g/L and the cells were grown till late exponential phase to 3.0 OD_{600}.

2.2. Cellular extraction procedure

Culture cells grown as described above were washed three times with cold H_2O_{dd} and suspended in 900 μL of cold methanol (−20 °C) to quench intracellular metabolism. In the meantime an aliquot of the cultures was washed and the wet weight calculated. To extract the metabolites the method reported in [25] was followed. The method allowed the separation of polar and organic phases, which were dried under N_2 flux and stored at −80 °C until NMR analysis.

2.3. Sample preparation for NMR analysis

The freeze-dried polar samples were re-dissolved in 600 μL of D_2O phosphate buffer solution (pH = 7.4) containing 2 mM sodium 3-(trimethylsilyl) propionate-2,2,3,3-d_4 (TSP) as ^1H NMR reference, and transferred to 5 mm NMR glass tubes for analysis. The organic phases were re-dissolved in 600 μL of $CDCl_3$ containing 2 mM hexamethyl-disiloxane (HMDSO) as an ^1H NMR reference.

2.4. NMR spectroscopy

^1H NMR spectra were acquired at 25 °C using a Bruker Avance III 400 spectrometer (Bruker BioSpin GmbH, Germany) equipped with a magnet operating at 9.4 Tesla, where the ^1H nucleus resonates at 400.13 MHz. The probe-head was a 5 mm diameter multinuclear PABBO BB-1H/D (Z108618/0044) equipped with z-gradient.

The pulse sequence adopted for spectra acquisition was a presaturation–single 90° detection pulse–acquire–delay sequence where the D1 relaxation delay was optimised to 2.5 s to allow the acquisition of 64 k data point in about 5.5 s, satisfying full relaxation conditions.

The length of the detection pulse was calibrated previously to the acquisition of each spectrum, the spectral width was set to 6009.62 Hz (15 ppm) and 64 scans were collected for each spectrum.

2.5. Data analysis

^1H NMR spectra were processed using the 1D-NMR Manager ver. 12.0 software (Advanced Chemistry Development, Inc., Toronto, Ontario, Canada).

The assignment of the peaks to specific metabolites was achieved by standard two-dimensional (2D)^1H-^1H total correlation spectroscopy (TOCSY), ^1H-^{13}C heteronuclear single quantum correlation (HSQC), and heteronuclear multiple bond correlation (HMBC) and confirmed using an internal library of compounds, in comparison with literature data [26–30].

On the basis of the quantified metabolites, it was possible to calculate the fatty acid content. Unsaturated fatty acids (UFA) were derived from the integral of the allylic protons resonating at 2.02 ppm; polyunsaturated fatty acids (PUFA) were represented by the sum of linoleic and linolenic acid contents and they were calculated from the integral of the signal referred to the terminal CH_3 resonating at 0.96 ppm and the diallylic CH_2 resonating at 2.76 ppm, respectively; monounsaturated fatty acids (MUFA) were calculated as UFA − PUFA; saturated fatty acids (SFA) were calculated subtracting UFA content from the integral's value of the signal representing the amount of all the fatty acids present in the sample, i.e. βCH_2 resonating at 1.59 ppm.

The acquired NMR spectra were manually phased and baseline corrected; polar and organic spectra were referenced to the chemical shift of the TSP or HMDSO methyl resonance at δ 0.00 and 0.055 ppm, respectively. The quantification of metabolites was obtained by comparison of the integrals of specific signals to the internal standard (TSP or HMDSO) integral.

Table 1
Yeast strains and real-time PCR primer sequences used in this study.

Strains	Genotype	Reference
CBS2359	*MAT*a	[19]
GG1600	Isogenic to CBS2359 except *acs1:: lox*P	[20]
GG1998	Isogenic to CBS2359 except *acs2::lox*P	[20]
PM6-7A	*MAT***a** *ade-T600 uraA1-1*	[21]
PM6-7A/*pdc1Δ*	Isogenic to PM6-7A except *Klpdc1::URA3*	[22]
PM6-7A/VV32	*MAT***a** *ade-T600 uraA1-1 rag4-1*	[23]
PM6-7A/VV30	*MAT***a** *ade-T600 uraA1-1 rag8-1*	[24]
PM6-7A/VV12	*MAT***a** *ade-T600 uraA1-1 rag12-1*	[21]

Primer sequences used in the real-time PCR experiments

	Forward	Reverse
KlFAS1	5′-TTGGTGGACAAGGTAACACC-3′	5′-CCAGGAGTCTTTTGTGGTTG-3′
KlFAS2	5′-TGAAGAGAGTTTACAAGGCC-3′	5′-TGGTGGAGTCCTTGTCCAAA-3′
KlFAD2	5′-AATTGGGTGGTTGGATCTAC-3′	5′-GCCGCCAAATTTATCATACC-3′
KlFAD3	5′-GGATGGTCCCATACTTTTCT-3′	5′-AACCACCAATTTGTTGGCCA-3′
KlOLE1	5′-GTGTGCCATTAAGACATGAG-3′	5′-AATTCTGTGTGAGTGACTCC-3′
KlACS1	5′-ATGAAGCTGATGAACCAGGT-3′	5′-AACAACGGAATGAATGGCAC-3′
KlACS2	5′-CGAATTGTTGAGACAGGTCT-3′	5′-CATCGACAACTCTTTCCTTC-3′
KlACT1	5′-AATGCAAACTGCTTCTCAAT-3′	5′-AACAGATGGATGGAACAAAG-3′

2.6. Statistical analysis

Multivariate data analysis was carried out using Unscrambler 9.8 Software (CAMO, Oslo, Norway). Spectral data were mean-centered and autoscaled before analysis. Principal components analysis (PCA) was used to explore inherent clustering, to identify outliers and significant metabolites in the separation between sample groups.

Unpaired Student's *t* test (univariate test) was also applied; a P value <0.05 was considered for a statistically significant difference between wild type and mutant samples.

2.7. Real-time PCR

RNAs were extracted through the hot phenol method as described in [31] and then digested with 2 U/μl DNAse I (Ambion). Three micrograms of each sample was reverse transcribed for 60 min at 37 °C using oligo dT and M-MLV reverse transcriptase (Applied Biosystem) according to manufacturer's instructions and then diluted to a final concentration of 50 ng/μl. For real-time PCR assay, each well contained 1 μl of cDNA used as template, SensiMix SYBR & Fluorescein Kit was purchased from Bioline, and the selective primers used (200 nM), designed with Primer3 software, are reported in Table 1. All samples were run in triplicate. I Cycler IQ Multicolor Real-Time Detection System (Biorad) was used for the analysis. The real-time PCR conditions included a denaturing step at 95 °C for 3 min followed by 40 cycles at 95 °C for 30 s, 55 °C for 30 s, and 75 °C for 45 s. Two cycles were included as final steps: one at 95 °C (1 min) and the other at the annealing temperature specific for each couple of primers used (1 min). Quantification was performed using a comparative C_T method (C_T = threshold cycle value). Briefly, the differences between the mean C_T value of each sample and the C_T value of the housekeeping gene (*KlACT1*) were calculated: $\Delta C_{Tsample} = C_{Tsample} - C_{TKlACT1}$. Final result was determined as $2^{-\Delta\Delta CT}$ where $\Delta\Delta C_T = \Delta C_{Tsample} - \Delta C_{Tcontrol}$.

2.8. Lipid droplet staining

Aliquots of 100 μl of cultures, grown in the condition specified above, were centrifuged and washed with PBS. Cells were then incubated with Nile Red (5 μg/ml) (Sigma) for 5 min in the dark, washed twice with PBS and observed with the ZEISS fluorescence microscope equipped with a rhodamine filter.

Table 2
Chemical shifts complete pattern of the metabolites assigned through the examination of 1D- and 2D-NMRspectra. "U" indicates metabolites not univocally assigned yet.

	Metabolites integrated	^{1}H chemical shift (ppm)
Amino acids	Isoleucine (Ile)	0.94(t), **1.02(d)**, 1.25, 1.46, 1.98, 3.69(t)
	Valine (Val)	1.00(d), **1.05(d)**, 2.27, 3.60
	Allo-threonine (Allo-Thr)	**1.20(d),** 3.97, 4.22
	Threonine (Thr)	**1.33(d)**, 3.58(d), 4.24(qui)
	Lysine (Lys)	1.48(m), 1.51, 1.73(m), 1.89, **3.04(t)**, 3.75(t)
	Alanine (Ala)	**1.48(d)**, 3.77(q)
	Aspartate (Asp)	2.68, **2.82(dd),** 3.88
	Histidine (His)	3.12(dd), 3.23(dd), 3.97, **7.06(s)**, 7.78(s)
	Tryptophane (Trp)	3.30(dd), 3.54(dd), 4.12, 7.20(dd), 7.28(dd), **7.32(s)**, 7.54(d), 7.74(dd)
	Glycine (Gly)	**3.56(s)**
Small organic acids	Butyrate (Btr)	**0.90(t)**, 1.56, 2.16(t)
	Isobutyrate (Iso-Btr)	**1.08(d)**, 2.39
	Lactate (Lac)	**1.33(d)**, 4.10(q)
	Glutamic acid (Glu)	2.07(dt) - 2.12(dt), **2.36(dt)**, 3.76(t)
	Malate (Mal)	2.37(dd), **2.67(dd)**, 4.30(dd)
	Succinate (Succ)	**2.41(s)**
	Fumarate (Fum)	**6.52(s)**
	Formate (For)	**8.46(s)**
Carbohydrates	α-Trehalose (Tre)	3.46(t), 3.66(dd), 3.75, 3.78, 3.84, 3.88, **5.20(d)**
	Myo-inositol (MI)	3.28(t), 3.52, 3.61, **4.06(t)**
	β-Glucose (β-Glc)	3.24, 3.46, 3.73, 3.88, **4.65(d)**
	α-Glucose (α-Glc)	3.41, 3.55, 3.70, 3.84,**5.24(d)**
Other hydro-soluble molecules	Orotidine 5-phosphate (OMP)	3.78, 3.87, 3.95, 4.35(t), 4.75, **5.55(d)**, 5.77(s)
	NAD	4.22, 4.24, 4.38, 4.43, 4.51(dd), 4.55, 4.81, 6.04(d), 6.09(d), 8.18(s), 8.20(t), 8.43(s), 8.84(dd), 9.15(d), **9.33(s)**
Unassigned hydro-soluble molecules	U1	**2.98(s)**
	U2	3.70, 4.11, 4.25, 4.31, **5.31(d)**
	U3	3.88, 4.01, 4.43, 4.78, **5.52(d)**
	U4	3.89, 4.04, 4.59, **4.97(t)**, 6.12(d)
	U5	**8.27(s)**
	U6	**8.31(s)**
	U7	**8.62(s)**
Fatty acids	Fatty acids	0.88(ωCH_3), 1.29($(CH_2)_n$), **1.59**(βCH_2) **2.02**(CH_2 allylic), 2.25(αCH_2), 2.80(CH_2 diallylic), 5.33(CH vinylic)
	ω_6 fatty ac. (LLA: linoleic acid)	0.89, 1.29(m), 1.59(m), 2.04, 2.27, **2.76(t)**, 5.32
	ω_3 fatty ac. (LNA: linolenic acid)	**0.96(t)**, 1.31, 1.59(m), 2.04, 2.32, 2.79(t), 5.33
Acyl-glycerols	1-MonoAcyl glycerols (MAG)	**3.59(dd)**, 3.69(dd), 3.92(m), 4.14(dd), 4.20(dd)
	DiAcyl glycerols (DAG)	**3.72(dd)**, 4.24(d/t), 5.06(dd)
	TriAcyl glycerols (TAG)	4.13, **4.36(dd)**, 5.24(dd)
Sterols	Ergosterol (Erg)	0.62(s), 0.81(d), 0.83(d), 0.91(d), 0.94(s), 1.03 (d),1.29(t), 1.47(m), 1.88(d), 2.04, 2.27(t/dd), 2.46, 3.63(m), 5.18(d), 5.20(d), 5.38(d), **5.56(d)**
Unassigned lipo-soluble molecules	U8	**1.42(s)**

Signals used for metabolites quantificafication were reported in bold; s, singlet; d, doublet; dd, double of doublets; t, triplet; dt, doublet of triplets; q, quartet; qui, quintet; m, multiplet.

3. Results

3.1. Metabolites profile in wild type and rag8 cells by ^{1}H-NMR spectroscopy

In order to analyze the metabolic changes taking place in *K. lactis rag* mutants, strains unable to grow under strictly fermentative conditions [6], we took advantage of the *rag8* mutant affected in the CKI activity and unable to tolerate osmostress [8].

To determine the best conditions for the metabolomic analysis by ^{1}H-NMR spectroscopy, growth curves of wild type and mutant strains were analyzed under different glucose concentrations (data not shown). An NMR-based metabolic profiling from aqueous and organic cellular extract phases was then generated from cells grown on glucose as specified in Materials and Methods.

In Table 2, the resonance assignments of the metabolites measured on polar and organic extracts are depicted based on the spectra reported in Fig. S1. The metabolite concentrations were measured and expressed as μmol g^{-1} wet weight (Fig. 1). Principal component analysis was performed to explore the data field. Component score plots showed a clear clustering between wild type and mutant samples (Fig. 2A). The first principal component (PC1), explaining 53% of the total variability, was responsible for this separation among *rag8* and wild type cells.

PC1 loadings plot, reported in Fig. 2B, showed the important variables in the separation among wild type and *rag8* group. Loadings

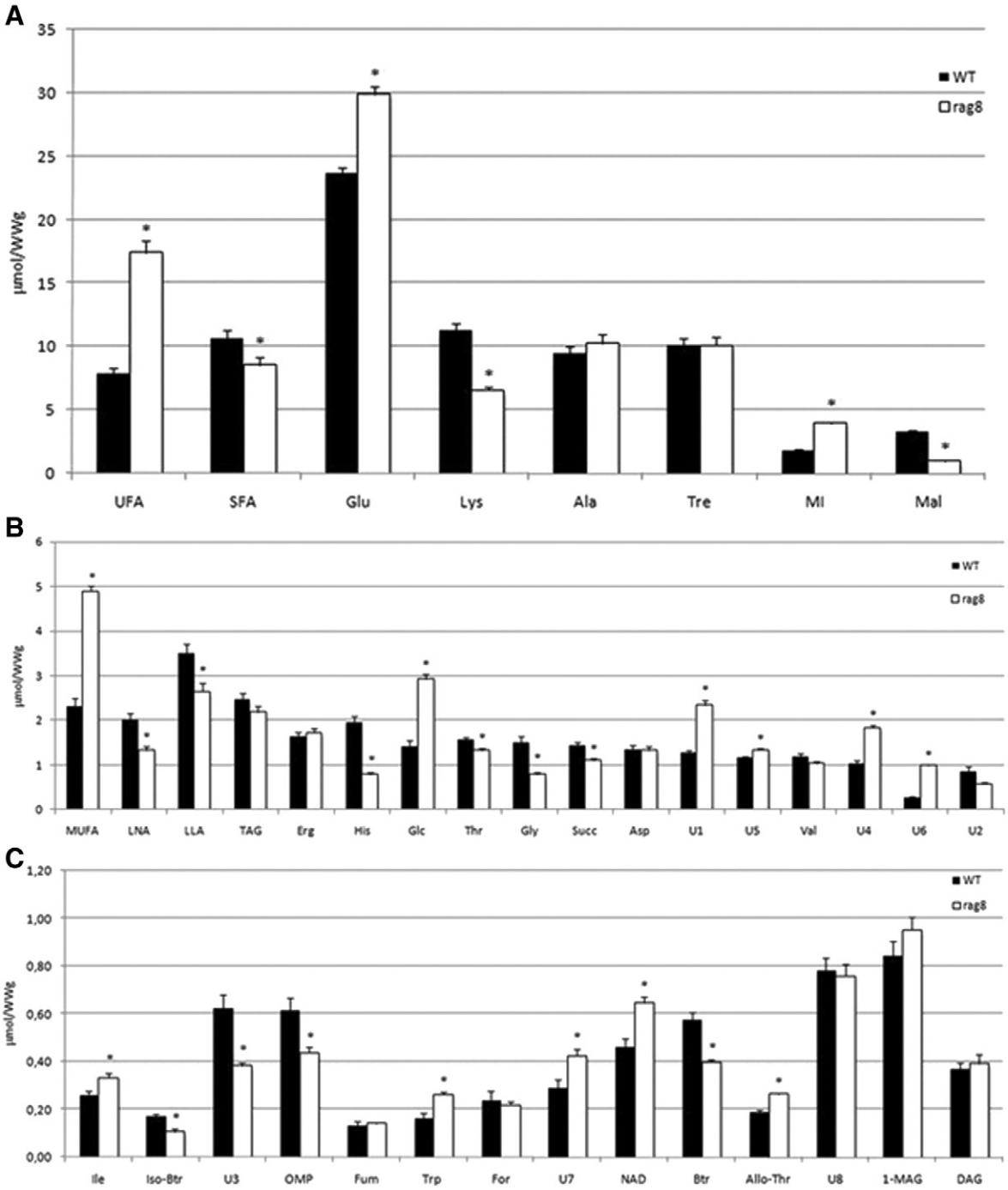

Fig. 1. Histograms relative to the concentrations of the metabolites present in (A) large and (B) intermediate amount or (C) in trace in hydro-alcoholic and chloroformic extracts. The stars indicate those metabolites whose variation in concentration between wild type and mutant cells is statistically significant, at a univariate Student's *t* test ($P < 0.05$).

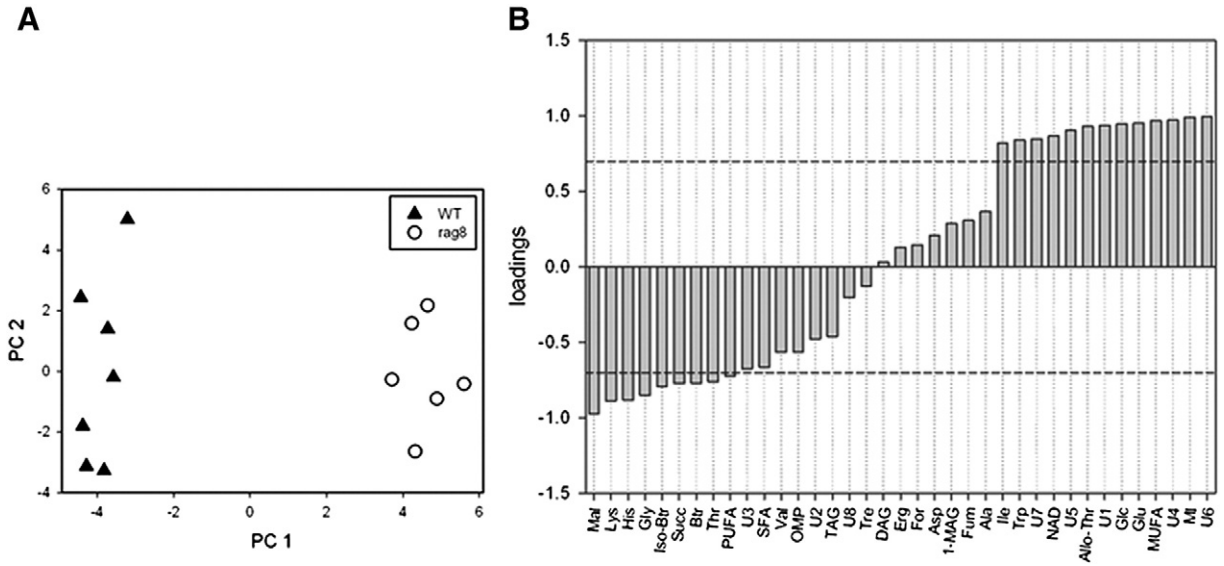

Fig. 2. (A) PCA scores plot relative to wild type and mutant samples. Total variability represented: 69% (PC1: 53%; PC2: 16%). (B) PCA loading values for each variable measured (metabolites) relative to PC1. Loadings above and under 0.7 and –0.7 were considered statistically significant at $P < 0.01$.

above and under 0.7 and –0.7 as Pearson's correlation coefficient values among original variables and PC1 were considered statistically significant at $P < 0.01$. The *rag8* mutant showed changes in several metabolite levels. Among the metabolites present in the mutant at higher concentrations, we observed a significant increase in the unsaturated fatty acid (UFA), glutamate (Glu) and myo-inositol (MI) levels and a decrease in the saturated fatty acids (SFA), lysine (Lys) and malate (Mal) level (Fig. 1A). Notably, the increase in UFAs observed in *rag8* cells was only limited to the mono-unsaturated fatty acids (MUFA) palmitoleic and oleic acid content. Conversely, the ω3 and ω6 linoleic (LLA) and linolenic (LNA) polyunsaturated fatty acids (PUFAs) showed, also by Student's *t* test, a statistically significant decrease (Fig. 1B).

Among the metabolites present at lower concentrations in the soluble fraction (Fig. 1B and C), glucose (Glc), isoleucine (Ile), tryptophan (Trp), allo-threonine (Allo-Thr) and nicotinamide adenine dinucleotide (NAD) were increased in *rag8*, as compared to the wild type strain, while histidine (His), glycine (Gly), succinate (Succ), isobutyrate (Iso-Btr), orotidine monophosphate (OMP) and butyrate (Btr) were reduced.

3.2. Real-time PCR analysis of genes involved in the synthesis of fatty acids

To determine if the different levels of fatty acids in *rag8* can be ascribed to mechanisms of regulation controlled at transcriptional levels, as compared to the wild type cells, we evaluated by real-time PCR analysis the expression profile of genes directly involved in their synthesis.

In *K. lactis* the expression of the two acetyl-coA (ac-CoA) synthase genes (*KlACS1* and *KlACS2*), the first step in the synthesis of fatty acids, like in *S. cerevisiae*, is differently regulated by carbon sources [32,33,20]. Real-time PCR analysis of these genes showed a highly reduced transcription of *ACS2* but not of *ACS1* in *rag8*, as compared to wild type cells (Fig. 3A).

Then, we analyzed *KlFAS1* and *KlFAS2*, the two genes coding for the two fatty acids synthetase activities responsible for the sequential addition of ac-CoA to the growing fatty acid, steps leading to the synthesis of the palmitic (16:0) and stearic (18:0) acids (SFAs). Despite the increased amounts of the whole fatty acid content (UFA + SFA) in the mutant (Fig. 1A), the levels of the two transcripts were dramatically reduced in *rag8*, as compared to wild type cells (Fig. 3A). Unexpected results were also obtained with the *OLE1*, *FAD2* and *FAD3* desaturase genes encoding the palmitate and stearate Δ9 desaturase the former and oleate Δ15 and linoleate Δ12 desaturase activities the latter two, respectively. Although MUFA contents are increased, whereas PUFAs are reduced in the mutant, real-time PCR analysis only showed slightly reduced levels of expression for the three genes in *rag8* cells as compared to the parental strain (Fig. 3A).

To test whether the reduced transcription of these genes in *rag8* belongs to a shared regulatory circuit common to all *rag* mutants, we performed the real-time PCR analysis on *rag4*, *rag6* and *rag12* mutant strains. The *RAG4* gene codes for the glucose sensor that together with *RAG8* controls the expression of the low affinity glucose transporter *RAG1* gene [34]. *RAG6* and *RAG12* code for the pyruvate decarboxylase and dl-glycerol-3-phosphatase, respectively, responsible for the production of acetaldehyde, an indispensable intermediate in the synthesis of ac-CoA, and glycerol, a compound required for the synthesis of phospholipids and for the resistance to osmostress. The results of this analysis showed that, also in these mutants although at lower extend, the expression of genes involved in the synthesis of fatty acids was down modulated similarly to *rag8* cells (Fig. 3B). However, the increased expression of *OLE1* observed in *rag6* and *rag12*, as compared to *rag4* and *rag8* mutants, can be explained by the direct role of these two genes in the synthesis of fatty acids/phospholipids.

To get insights on the genetic interaction between glucose metabolism and fatty acids synthesis, a phenotypic analysis of both *ACS* deletion mutants was performed. Indeed, as shown in Fig. 3C, a *rag* phenotype was found in the case of cells depleted of *KlACS2*. These cells, in fact, were unable to grow in the presence of antimycin A or osmotic stress conditions (in e.g. NaCl), similarly to *rag6* and *rag8* mutant strains, reported as a control.

3.3. Lipid droplet analysis of wild type and rag8 cells by Nile Red staining

Recently, in *S. cerevisiae* the two casein kinases CKB1 and CKB2 were found involved in the size of lipid droplets (LDs), dynamic organelles that govern the storage, trafficking and turnover of lipids [35–37]. All LDs comprise a core of neutral lipids storage, i.e. triacylglycerols (TAG) and sterol esters (SE) wrapped by a monolayer of phospholipids containing embedded proteins. An investigation of LDs, by Nile Red staining, was performed on wild type and mutant cells taking into account the altered glycerol homeostasis in the *rag8* as well as the altered fatty acid amount [8]. A reduced amount of the LDs, also associated to lower fluorescence emission, was observed in *K. lactis*

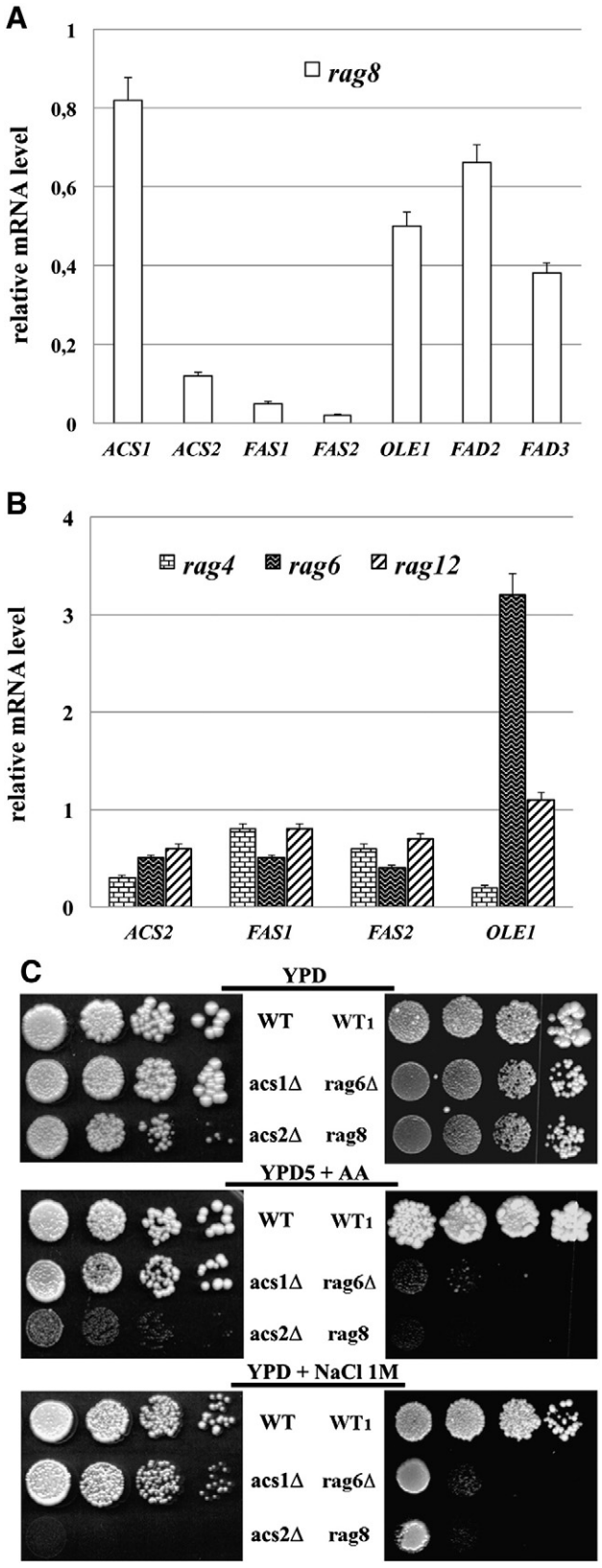

Fig. 3. (A and B) Expression of *ACS*, *FAS*, *OLE1* and *FAD* genes in wild type and *rag* mutant cells. Histograms show expression of fatty acids related genes detected by real-time PCR. Wild type levels were set to 1 (100%). (C) Growth test of wild types and *rag* mutants. CBS2359 (WT), PM6-7A (WT_1), *acs1* Δ *acs2*Δ *rag6* Δ and *rag8* strains were grown on YPD plate with/without antimycin A (YPD + AA) or NaCl 1 M (YPD + NaCl). Cultures, grown on YPD till late exponential phase, were adjusted to the same density and 5 μl of serial 10-fold dilutions was spotted onto the indicated medium. The initial concentration was 1×10^7 cells ml^{-1}.

cells depleted of the CKI activity, as compared to the wild type counterpart (Fig. 4). On average fewer lipid droplets were observed in *rag8* cells (90 LDs/100 cells) than in wild-type cells (240 LDs/100 cells). This difference in lipid droplet number between the two strains was statistically significant ($P < 0.01$, Student's t test). Notably, more than 30% of *rag8* cells resulted negative to Nile red staining.

4. Discussion

The study of the *rag8* strain can be regarded as a model for the metabolic adaptation of *rag* mutants. The *rag8* mutant is 1 of at least 19 complementation groups harboring the Rag^- phenotype. The genetic dissection of this phenotype allowed the isolation of genes coding for glycolytic enzymes, activities involved in the utilization and sensing of glucose, cell cycle [8].

The determinations of the metabolites in *rag8* and wild type cells allowed the construction, on statistical basis, of a metabolic net interconnecting these compounds in mitochondria, endoplasmic reticulum (ER) and peroxisome organelles (Fig. 5). Metabolites data comparison between these two strains led us to the conclusions that the levels of metabolic intermediates produced in pathways generating the NADH/NADPH cofactors were decreased (Fig. 5 blue balls), while those associated with cofactors reoxidation routes were increased (red balls).

The altered values of these metabolites in the *rag8* strain could be interpreted as an obligate stress response of the mutant, to re-adjust the intra-cellular redox balance. Moreover, the increased contents of tryptophan and NAD^+ in the mutant also suggested the activation of pathways leading to the *de novo* synthesis of NAD to overcome the excessive generation of cytoplasmic NAD(P)H (Fig. 5).

This metabolic profile of *rag8* cells was in agreement with the observations that all *rag* mutants were characterized by reduced glucose utilization, reduced production of ethanol and the inability to accumulate/produce glycerol [8]. Yeast cells produce and accumulate ethanol and glycerol during fermentation for redox balancing and osmoregulation [38]. Therefore, the impaired glycolytic flux of *rag* mutants [6,39] is unable to support the accumulation of ethanol and glycerol for the cytoplasmic reoxidation of the NAD(P)H redox excess [40]. The metabolism of these cells becomes respiro-fermentative [4] and the respiratory chain is required for the neutralization of the NAD(P)H excess [41]. It follows that the addition of antimycin A, blocking the respiratory chain, inhibits the growth of these mutants [6].

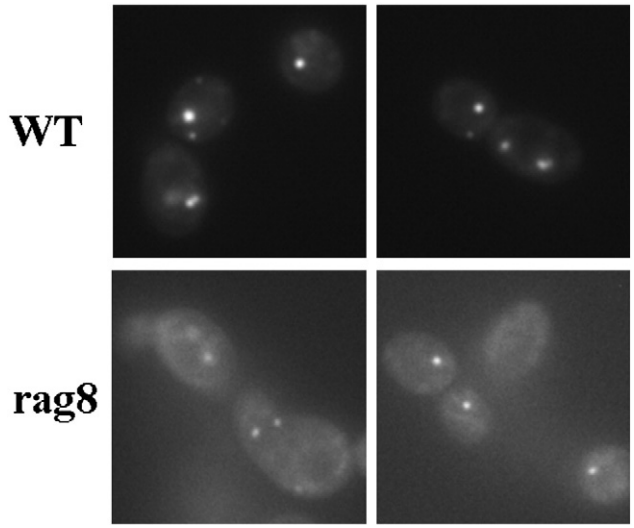

Fig. 4. Fluorescence micrographs (100×) of lipid droplets of wild type and mutant cells stained with Nile Red.

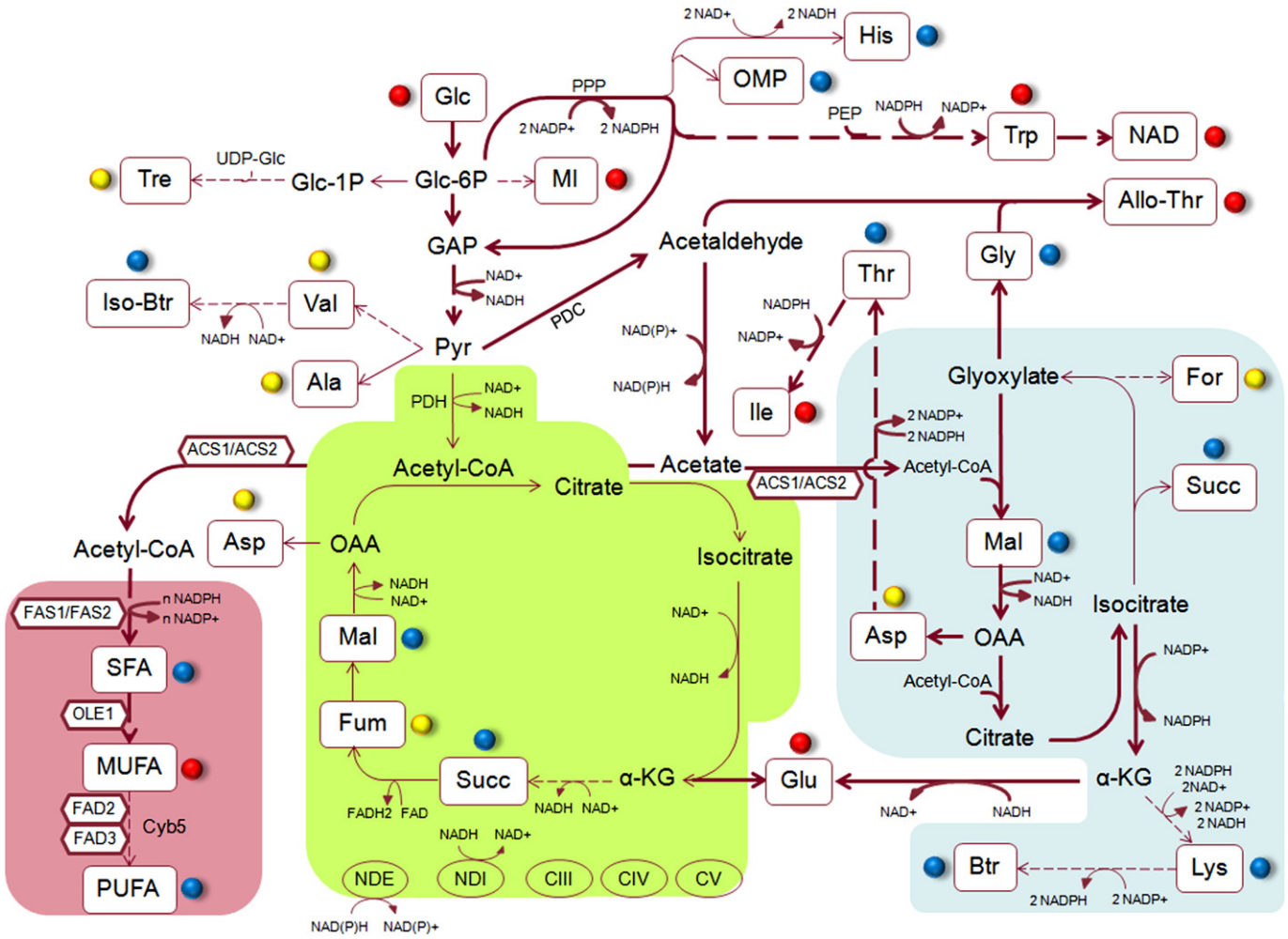

Fig. 5. Metabolic network. Colored balls denote mutant metabolite level changes in respect to wild type samples: red balls indicate metabolites present in higher amount, blue balls metabolites in lower amount and yellow balls metabolites which did not significantly vary. Figure also displays the main cell compartments in which the occurring reactions are expected: mitochondria (light green), endoplasmatic reticulum (pink) and peroxisome (light blue). Hexagons near the reaction arrows reported the genes discussed.

Moreover, *rag* mutants display a respiratory utilization of glucose mainly through the pentose phosphate pathway with production of NADPH [6,4,41,42]. Indeed, differently from *S. cerevisiae* where NADPH accumulation is toxic/inhibitory for cell growth, as reported for the phosphoglucose isomerase *pgi1* mutant unable to grow in glucose medium [43], the corresponding *K. lactis rag2* mutant is capable of growing in glucose [6]. In fact, in *K. lactis* Nde1 and Nde2, the single rotenone-insensitive inner mitochondrial-membrane activities facing the outer membrane can accept both NADPH and NADH as substrate (Fig. 5) [44]. These activities, which can reoxidize both cytoplasmic cofactors feeding the respiratory chain through the ubiquinone [44,42], are probably essential for the survival of all *rag* mutants.

The levels of OMP, an intermediate in the *de novo* synthesis of pyrimidine, appeared in agreement with the presence in both strains of the *ura3* mutation that blocks the biosynthesis of uracyl leading to OMP accumulation. Since Yck1 and Yck2 in *S. cerevisiae* control uracyl permease [17], the reduced level of OMP in *rag8* concords with the CKI depletion, suggesting a decreased uptake of uracyl in the presence of an altered pyrimidine biosynthesis.

On the other hand, the lower amounts of malate and succinate, produced/exchanged by the glyoxylate and the Krebs cycles, and the increased content of glutamate and allo-threonine, determined in *rag8* cells, suggested rerouting/reduced refurbishing of ac-CoA to these organelles (Fig. 5). Indeed, the increased level of allo-threonine, determined by the condensation of acetaldehyde with glycine, can be explained by a slightly reduced conversion of acetaldehyde to acetate. A plain conversion of all the aldehyde to acetate by aldehyde dehydrogenase would lead to a further excessive production of NAD(P)H (Fig. 5) [42], a condition that mutant cells probably avoid favoring its partial conversion to allo-threonine to the detriment of ac-CoA final content.

Ac-CoA is a key intermediate in cellular metabolism for energy generation in the mitochondria, for histone acetylation in the nucleus, for fatty acids β-oxidation in the peroxisome and for the synthesis of fatty acids in the ER. Ac-CoA, produced in the Krebs cycle from pyruvate or by the condensation of acetate with the coenzyme A by the *KlACS1* and *KlACS2* genes products (Fig. 5), is compartmentalized and its content varies with nutrient sources. Indeed, the regulation of the two *K. lactis* genes, identical to that of *ACS1* and *ACS2* of *S. cerevisiae* [45,46], could lead to the potential asymmetric distribution of ac-CoA between these organelles. In fact, *ACS1* is subjected to glucose inactivation and is preferentially expressed on non-fermentable carbon sources, whereas *ACS2* is induced on glucose–ethanol/anaerobic conditions [32,33,20]. Transcription analysis confirmed these data showing highly reduced levels of transcription of *ACS2*, as compared to *ACS1* (Fig. 3), not only in *rag8* but also in *rag4, rag6* and *rag12* (Fig. 3B), suggesting, together with the increased content of allo-threonine, a reduced content/unequal distribution of ac-CoA between cellular compartments in mutant cells.

The higher MUFA content in *rag8* cells, observed in the presence of a highly reduced expression of the fatty acids synthetase *FAS1* and *FAS2* genes, (Fig. 3), is also part of the obligate unequal distribution of

ac-CoA response to the different compartments, and to compensate the high NAD(P)H/NAD(P)$^+$ ratio determined by the increased glucose flux through the pentose phosphate pathway. Moreover, *rag8* transcriptional data seems to be extended to other *rag* mutants, confirming that a common pathway regulates glucose utilization and the metabolism of fatty acids necessary for the stress response. In support of this view the *acs2* strain, herein identified as a new *rag* mutant, resulted to be sensitive to NaCl, demonstrating that the initial step for the synthesis of fatty acids has a central role in this pathway. Conversely, the highly increased levels of *OLE1* mRNA in *rag6* and *rag12* suggested either its control by the glycolytic flux, interrupted in these two mutants, or a direct regulatory role of these two genes on its expression. The slightly higher levels of *FAS1* and *FAS2* in *rag4*, *rag6* and *rag12*, as compared to *rag8*, suggested that CKI has a major regulatory control role on genes involved in the stress response pathway.

In contrast to the MUFA contents, in *rag8* cells the synthesis of PUFAs is decreased. The levels of *FAD2* and *FAD3* mRNA, coding for the Δ12 and Δ15 fatty acid desaturase activities, are reduced although at lower extent than the transcripts of *FAS1* and *FAS2* genes required for the initial synthesis of all fatty acids (Fig. 3). These results thus suggested a blockage of the Δ12 and Δ15 fatty acid desaturase activities at post-traductional levels but not that of the Δ9 desaturase Ole1 enzyme (see Fig. 5). Differently from the Ole1 desaturase, which harbors a cytochrome domain, the expression of the cytochrome b5 gene *CYB5* is crucial for the synthesis of these PUFAs by Fad2 and Fad3. In fact, [47] reported that in *S. cerevisiae* higher levels of PUFAs synthesis, occurring when the *K. lactis FAD2* and *FAD3* genes are expressed in this yeast, require the contemporary co-expression of the *CYB5* gene. Cyb5 accelerates the electron transfer from the NADH cofactor to the fatty acid, which is necessary to introduce the double bond by the desaturases [48]. Although more experiments will be necessary to confirm the role of Cyb5 also in *K. lactis*, we could attribute its putative lower amounts to the reduced levels of Ac-CoA, glycine and succinate (through succinyl-CoA) observed in *rag8* cells, mitochondrial and cytoplasmic precursors that are required for the synthesis of the prosthetic heme group of cytochromes.

Fatty acids, together with phospholipids, sphingolipids and ergosterol, are plasma membrane building blocks [49] influencing several important biological aspects of membrane functions, such as fluidity and permeability [50]. Since these lipid biosynthetic pathways are linked by regulatory mechanisms [51,52], a major role of CKIs in the control of these processes has been reported in *S. cerevisiae* [13,15].

Therefore, the reduced amount of LDs, observed in Rag8 depleted cells by the Nile Red assay (Fig. 4), could be in agreement with a decreased membrane lipid turnover/loss of the fatty acids/phospholipids vesicles dynamic balance between biosynthetic and oxidation processes in different cellular compartments (Fig. 5). In contrast, the similar ergosterol content determined in the two strains suggested that Rag8 is not involved in the control of its synthesis (Fig. 1B).

Finally, we also found accumulation of intracellular glucose in mutant cells (Fig. 1B). In view of the fact that glucose assumption from the medium was about 20% of the total for both strains (data not shown), in the presence of a reduced glycolytic flux [39], we can speculate that its higher intracellular concentration, together with myo-inositol (Fig. 1A), had osmotic adaptive role in cells unable to produce/accumulate glycerol [8].

Supplementary data to this article can be found online at http://dx.doi.org/10.1016/j.bbagen.2013.10.020.

Acknowledgements

This work was funded by “Ateneo 2012” – Sapienza University of Rome. EZ was the recipient of a Pasteur Institute, Cenci Bolognetti Foundation “Teresa Ariaudo” fellowship. The authors would like to thank Dr. Giorgio Capuani for assistance to multivariate analysis and G.P.H. van Heusden (Leiden University) for providing the *acs* strains.

References

[1] D.H. Lackner, M.W. Schmidt, S. Wu, D.A. Wolf, J. Bähler, Regulation of transcriptome, translation, and proteome in response to environmental stress in fission yeast, Genome Biol. 13 (2012) 1–14.
[2] R. Rodicio, J.J. Heinisch, Yeast on the milky way: genetics, physiology and biotechnology of *Kluyveromyces lactis*, Yeast 30 (2013) 165–177.
[3] R.H. De Deken, The Crabtree effect: a regulatory system in yeast, J. Gen. Microbiol. 44 (1966) 149–156.
[4] M.I. Gonzalez-Siso, M.A. Freire-Picos, E. Ramil, M. Gonzalez- Domınguez, A. Rodrıguez Torres, M.E. Cerdàn, Respirofermentative metabolism in *Kluyveromyces lactis*: insights and perspectives, Enzyme Microb. Technol. 26 (2000) 699–705.
[5] A. Merico, S. Galafassi, J. Piskur, C. Compagno, The oxygen level determines the fermentation pattern in *Kluyveromyces lactis*, FEMS Yeast Res. 9 (2009) 749–756.
[6] P. Goffrini, A.A. Algeri, C. Donnini, M. Wésolowski-Louvel, I. Ferrero, *RAG1* and *RAG2*: nuclear genes involved in the dependence/independence on mitochondrial respiratory function for growth on sugars, Yeast 5 (1989) 99–106.
[7] M. Wésolowski–Louvel, C. Prior, D. Bornecque, H. Fukuhara, Rag2 mutations involved in glucose metabolism in yeast: isolation and genetic characterization, Yeast 8 (1992) 711–719.
[8] S. Cialfi, D. Uccelletti, A. Carducci, M. Wésolowski-Louvel, P. Mancini, H.J. Heipieper, M. Saliola, KlHsl1 is a component of glycerol response pathways in the milk yeast *Kluyveromyces lactis*, Microbiology 157 (2011) 1509–1518.
[9] J. Blaisonneau, H. Fukuhara, M. Wésolowski-Louvel, The *Kluyveromyces lactis* equivalent of casein kinase I is required for the transcription of the gene encoding the low-affinity glucose permease, Mol. Gen. Genet. 253 (1997) 469–477.
[10] H. Neil, M. Hnatova, M. Wesolowski-Louvel, A. Rycovska, M. Lemaire, Sck1 activator coordinates glucose transport and glycolysis and is controlled by Rag8 casein kinase I in *Kluyveromyces lactis*, Mol. Microbiol. 63 (2007) 1537–1548.
[11] A.J. DeMaggio, R.A. Lindberg, T. Hunter, M.F. Hoekstra, The budding yeast HRR25 gene product is a casein kinase I isoform, Proc. Natl. Acad. Sci. U. S. A. 89 (1992) 7008–7012.
[12] L.C. Robinson, E.J. Hubbard, P.R. Graves, A.A. DePaoli-Roach, P.J. Roach, C. Kung, D.W. Haas, C.H. Haqedorn, M. Goebl, M.R. Culbertson, Yeast casein kinase I homologues: an essential gene pair, Proc. Natl. Acad. Sci. U. S. A. 89 (1992) 28–32.
[13] X. Wang, M.F. Hoekstra, A.J. DeMaggio, N. Dhillon, A. Vancura, J. Kuret, G.C. Johnston, R.A. Singer, Prenylated isoforms of yeast casein kinase I, including the novel Yck3p, suppress the gcs1 blockage of cell proliferation from stationary phase, Mol. Cell. Biol. 10 (1996) 5375–5385.
[14] L.C. Robinson, M.M. Menold, S. Garrett, M.R. Culbertson, Casein kinase I-like protein kinases encoded by *YCK1* and *YCK2* are required for yeast morphogenesis, Mol. Cell. Biol. 13 (1993) 2870–2881.
[15] H.R. Panek, J.D. Stepp, H.M. Engle, K.M. Marks, P.K. Tan, S.K. Lemmon, L.C. Robinson, Suppressors of *YCK*-encoded yeast casein kinase 1 deficiency define the four subunits of a novel clathrin AP-like complex, EMBO J. 16 (1997) 4194–4204.
[16] E. Estrada, P. Agostinis, J.R. Vandenheede, J. Goris, W. Merlevede, J. François, A. Goffeau, M. Ghislain, Phosphorylation of yeast plasma membrane H + -ATPase by casein kinase I, J. Biol. Chem. 271 (1996) 32064–32072.
[17] C. Marchal, R. Haguenauer-Tsapis, D. Urban-Grimal, Casein kinase I-dependent phosphorylation within a PEST sequence and ubiquitination at nearby lysines signal endocytosis of yeast uracil permease, J. Biol. Chem. 275 (2000) 23608–23614.
[18] A.R. Reddi, V.C. Culotta, *SOD1* integrates signals from oxygen and glucose to repress respiration, Cell 152 (2013) 224–235.
[19] CBS-KNAW Fungal Biodiversity Centre, URL: http://www.cbs.knaw.nl/.
[20] A.M. Zeeman, H.Y. Steensma, The acetyl co-enzyme A synthetase genes of *Kluyveromyces lactis*, Yeast 20 (2003) 13–23.
[21] M. Wésolowski-Louvel, P. Goffrini, I. Ferrero, H. Fukuhara, Glucose transport in the yeast *Kluyveromyces lactis*, Mol. Gen. Genet. 233 (1992) 89–96.
[22] M. Bianchi, L. Tizzani, M. Destruelle, L. Frontali, M. Wésolowski-Louvel, The ‘petite-negative’ yeast *Kluyveromyces lactis* has a single gene expressing pyruvate decarboxylase activity, Mol. Microbiol. 19 (1996) 27–36.
[23] S. Betina, P. Goffrini, I. Ferrero, M. Wésolowski-Louvel, *RAG4* gene encodes a glucose sensor in *Kluyveromyces lactis*, Genetics 158 (2001) 541–548.
[24] J. Blaisonneau, H. Fukuhara, M. Wésolowski-Louvel, The *Kluyveromyces lactis* equivalent of casein kinase I is required for the transcription of the gene encoding the low-affinity glucose permease, Mol. Gen. Genet. 253 (1997) 469–477.
[25] A. Miccheli, T. Aureli, M. Delfini, M.E. Di Cocco, P. Viola, R. Gobetto, F. Conti, Study on the influence of inactivation enzyme techniques and extraction procedures on cerebral phosphorylated metabolite levels by P-31 NMR spectroscopy, Cell. Mol. Biol. 34 (1988) 591–603.
[26] W.M.T. Fan, Metabolite profiling by one- and two-dimensional NMR analysis of complex mixtures, Prog. Nucl. Magn. Reson. Spectrosc. 28 (1996) 161–219.
[27] M.A. Brescia, V. Mazzilli, A. Sgaramella, S. Ghelli, F.P. Fanizzi, A. Sacco, 1H-NMR characterization of milk lipids: a comparison between cow and buffalo milk, JAOCS 81 (2004) 431–436.
[28] W.M.T. Fan, A.N. Lane, Structure-based profiling of metabolites and isotopomers by NMR, Prog. Nucl. Magn. Reson. Spectrosc. 52 (2008) 69–117.
[29] D. Capitani, L. Mannina, N. Proietti, A.P. Sobolev, A. Tomassini, A. Miccheli, M.E. Di Cocco, G. Capuani, R. De Salvador, M. Delfini, Monitoring of metabolic profiling and water status of Hayward kiwifruits by nuclear magnetic resonance, Talanta 82 (2010) 1826–1838.
[30] M. Massimi, A. Tomassini, F. Sciubba, A.P. Sobolev, L. Conti Devirgiliis, A. Miccheli, Effects of resveratrol on HepG2 cells as revealed by 1H-NMR based metabolic profiling, Biochim. Biophys. Acta 1820 (2012) 1–8.
[31] E. Zanni, M. Franco, M. Nakano, H. Iida, C. Palleschi, D. Uccelletti, *KlMID1*, a relevant key player between endoplasmic reticulum homeostasis and mitochondrial dysfunction in *Kluyveromyces lactis*, Microbiology 158 (2012) 1694–1701.

[32] A.M. Zeeman, M. Kuyper, J.T. Pronk, J.P. van Dijken, H.Y. Steensma, Regulation of pyruvate metabolism in chemostat cultures of *Kluyveromyces lactis* CBS 2359, Yeast 16 (2000) 611–620.
[33] T. Lodi, M. Saliola, C. Donnini, P. Goffrini, Three target genes for the transcriptional activator Cat8p of *Kluyveromyces lactis*: acetyl coenzyme A synthetase genes *KlACS1* and *KlACS2* and lactate permease gene *KlJEN1*, J. Bacteriol. 183 (2001) 5257–5261.
[34] X.J. Chen, M. Wésolowski-Louvel, H. Fukuhara, Glucose transport in the yeast *Kluyveromyces lactis*. II. Transcriptional regulation of the glucose transporter gene *RAG1*, Mol. Gen. Genet. 233 (1992) 97–105.
[35] K. Athenstaedt, G. Daum, The life cycle of neutral lipids: synthesis, storage and degradation, Cell. Mol. Life Sci. 63 (2006) 1355–1369.
[36] W. Fei, G. Shui, Y. Zhang, N. Krahmer, C. Ferguson, T.S. Kapterian, R.C. Lin, I.W. Dawes, A.J. Brown, P. Li, X. Huang, R.G. Parton, M.R. Wenk, T.C. Walther, H. Yang, A role for phosphatidic acid in the formation of "supersized" lipid droplets, PLoS Genet. 7 (2011) 1–11.
[37] T.C. Walther, R.V. Jr Farese, Lipid droplets and cellular lipid metabolism, Annu. Rev. Biochem. 81 (2012) 687–714.
[38] S. Hohmann, Control of high osmolarity signalling in the yeast *Saccharomyces cerevisiae*, FEBS Lett. 583 (2009) 4025–4029.
[39] M. Lemaire, M. Wesolowski–Louvel, Enolase and glycolytic flux play a role in the regulation of the glucose permease gene *RAG1* of *Kluyveromyces lactis*, Genetics 168 (2004) 723–731.
[40] J.P. van Dijken, W.A. Scheffers, Redox balances in the metabolism of sugars by yeast, FEMS Microbiol. Rev. 32 (1986) 199–224.
[41] K.M. Overkamp, B.M. Bakker, H.Y. Steensma, J.P. van Dijken, J.T. Pronk, Two mechanisms for oxidation of cytosolic NADPH by *Kluyveromyces lactis* mitochondria, Yeast 19 (2002) 813-624.
[42] M. Saliola, A. Tramonti, C. Lanini, S. Cialfi, D. De Biase, C. Falcone, Intracellular NADPH levels affect the oligomeric state of the glucose 6-phosphate dehydrogenase, Eukaryot. Cell. 11 (2012) 1503–1511.
[43] E. Boles, W. Lehnert, F.K. Zimmermann, The role of the NAD-dependent glutamate dehydrogenase in restoring growth on glucose of a *Saccharomyces cerevisiae* phosphoglucose isomerase mutant, Eur. J. Biochem. 217 (1993) 469–477.
[44] N. Tarrio, S. Diaz Prado, M.E. Cerdan, M.I. Gonzalez Siso, The nuclear genes encoding the internal (*KlNDI1*) and external (*KlNDE1*) alternative NAD(P)H:ubiquinone oxidoreductases of mitochondria from *Kluyveromyces lactis*, Biochim. Biophys. Acta 1707 (2005) 199–210.
[45] M.A. van den Berg, P. de Jong-Gubbels, C.J. Kortland, J.P. van Dijken, J.T. Pronk, H.Y. Steensma, The two acetyl-coenzyme A synthetases of *Saccharomyces cerevisiae* differ with respect to kinetic properties and transcriptional regulation, J. Biol. Chem. 271 (1996) 28953–28959.
[46] Y. Chen, V. Siewers, J. Nielsen, Profiling of cytosolic and peroxisomal acetyl-CoA metabolism in *Saccharomyces cerevisiae*, PLoS One 7 (2012) 1–9.
[47] H. Yazawa, H. Iwahashi, Y. Kamisaka, K. Kimura, H. Uemura, Improvement of polyunsaturated fatty acids synthesis by the co-expression of *CYB5* with desaturase genes in *Saccharomyces cerevisiae*, Appl. Microbiol. Biotechnol. 87 (2010) 2185–2193.
[48] D.C. Lamb, D.E. Kelly, N.J. Manning, M.A. Kaderbhai, S.L. Kelly, Biodiversity of the P450 catalytic cycle: yeast cytochrome b5/NADH cytochrome b5 reductase complex efficiently drives the entire sterol 14-demethylation (CYP51) reaction, FEBS Lett. 462 (1999) 283–288.
[49] M.E. van der Rest, A.H. Kamminga, A. Nakano, Y. Anraku, B. Poolman, W.N. Konings, The plasma membrane of *Saccharomyces cerevisiae*: structure, function, and biogenesis, Microbiol. Mol. Biol. Rev. 59 (1995) 304–322.
[50] J.K. Volkman, Sterols in microorganisms, Appl. Microbiol. Biotechnol. 60 (2003) 495–506.
[51] M. Veen, C. Lang, Interactions of the ergosterol biosynthetic pathway with other lipid pathways, Biochem. Soc. Trans. 33 (2005) 1178–1181.
[52] F. Mantzouridou, M.Z. Tsimidou, Observations on squalene accumulation in *Saccharomyces cerevisiae* due to the manipulation of *HMG2* and *ERG6*, FEMS Yeast Res. 10 (2010) 699–707.